MEIER, W. M. & OLSON, D. H. (1987). *Atlas of Zeolite Structure Types*. Washington, DC: Butterworth.
MESSERSCHMIDT, A. & PFLUGRATH, J. W. (1987). *J. Appl. Cryst.* **20**, 306–315.
Molecular Structure Corporation (1985). *TEXSAN. TEXRAY Structure Analysis Package*. Molecular Structure Corporation, 3200A Research Forest Drive, The Woodlands, Texas, USA.
MOTHERWELL, W. D. S. & CLEGG, W. (1978). *PLUTO*. Program for plotting molecular and crystal structures. Univ. of Cambridge, England.
NARDINI, G., RANDACCIO, L., KAUČIČ, V. & RAJIĆ, N. (1991). *Zeolites*, **11**, 192–194.
PAPIZ, M. Z. (1989). Personal communication.
PAPIZ, M. Z., ANDREWS, S. J., DAMAS, A. M., HARDING, M. M. & HIGHCOCK, R. M. (1990). *Acta Cryst.* C**46**, 172–173.
PARISE, J. B. (1986). *Acta Cryst.* C**42**, 670–673.
RAJIĆ, N., KAUČIČ, V. & STOJAKOVIĆ, D. (1990). *Zeolites*, **10**, 169–173.
RIZKALLAH, P. J., HARDING, M. M., LINDLEY, P. F., AIGNER, A. & BAUER, A. (1990). *Acta Cryst.* B**46**, 262–266.
SHELDRICK, G. M. (1976). *SHELX*. Program for crystal structure determination. Univ. of Cambridge, England.
SHELDRICK, G. M. (1986). *SHELXS*. Program for crystal structure solution. Univ. of Göttingen, Germany.
VASOVIC, D. & STOJAKOVIC, D. (1988). *J. Non-Cryst. Solids*, **109**, 129.

Acta Cryst. (1993). B**49**, 420–428

A Two-Wavelength Crystallographic Study of a New Aluminophosphate Containing Nickel

BY M. HELLIWELL AND B. GALLOIS*

Department of Chemistry, University of Manchester, Manchester M13 9PL, England

B. M. KARIUKI

Chemistry Department, Liverpool University, PO Box 147, Liverpool L69 3BX, England

V. KAUČIČ

Department of Chemistry and Chemical Technology, University of Ljubljana, 61000 Ljubljana, Slovenia, and Boris Kidrič Institute of Chemistry, 61000 Ljubljana, Slovenia

AND J. R. HELLIWELL

Department of Chemistry, University of Manchester, Manchester M13 9PL, England, and SERC Daresbury Laboratory, Warrington WA4 4AD, England

(*Received* 1 *July* 1992; *accepted* 14 *October* 1992)

Abstract

This paper describes the structure of a new aluminophosphate containing nickel. A single crystal of $NiAl_3P_4O_{18}C_4H_{21}N_4$ was used to collect data at Cu $K\alpha$ and Mo $K\alpha$ wavelengths on rotating-anode (Rigaku AFC-5R) and sealed-tube (Rigaku AFC-6S) diffractometers, respectively. The monoclinic unit cell was (for Cu $K\alpha$) $a = 10.0209\ (8)$, $b = 15.661\ (1)$, $c = 14.0914\ (8)$ Å, $\beta = 101.216\ (5)°$, space group $P2_1/n$. Determination of the structure showed that a novel arrangement had been formed, in which nickel occupied an octahedral site in the framework. The elemental analysis confirmed the presence of nickel. The Ni atom is coordinated to two framework O atoms and one water molecule. In addition, two template molecules of ethylenediamine are coordinated to the Ni atom, one monodentate and the other bidentate. The framework also contains three Al atoms and four P atoms that are all tetrahedrally bound to oxygen. A free water molecule is contained in the pores and is hydrogen bonded to the framework. The overall structure consists of aluminophosphate layers linked through Ni atoms. The crystal used for data collection was small ($0.02 \times 0.05 \times 0.25$ mm), but with the Cu $K\alpha$ data it was possible to refine all non-H atoms anisotropically to a final R (on F) of 0.057, $wR = 0.081$, with 3497 observed reflections having $I > 3\sigma(I)$ and 309 variables. Using the weaker Mo $K\alpha$ data, the final agreement factors were $R = 0.050$ and $wR = 0.055$, with 1057 observed reflections and 177 parameters. Between Cu $K\alpha$ and Mo $K\alpha$ wavelengths, the difference in f' is -3.32 e for nickel *versus* 0.15 e for aluminium (*i.e.* a ratio of 24). An f' difference Fourier electron-density map, based on phases calculated excluding the Ni atom,

* On leave from Laboratoire de Cristallographie, Université de Bordeaux, Talence, France.

0108-7681/93/030420-09$06.00

revealed a single peak of six times the r.m.s. value at the six-coordinate site, which is further evidence that nickel, rather than aluminium, is indeed present at this site.

1. Introduction

New microporous materials based on the aluminophosphate lattice have in recent years been the subject of intense investigations. They are characterized by pronounced structural diversification and more than two dozen structural types have been reported (Bennett, Dytrych, Pluth, Richardson & Smith, 1986). The data for their structural characterization are still scarce; one of the reasons for this is probably that large single crystals are difficult to obtain. Some structural types are named on the basis of their similarity to known zeolite structures, whilst other structures are completely new and have no zeolite analogues. The substitution of metallic elements into the neutral aluminium–phosphorus framework during synthesis gives rise to novel acidic and catalytic properties, the previously uncharged frameworks being unable to function as solid acid catalysts. Thus, metal-substituted aluminophosphates have been prepared for several of the first transition series and in some cases – MnAPO-11 (Pluth, Smith & Richardson, 1988) and CoAPO-*n* [*n* = 44, 47, 50 (Bennett & Marcus, 1988), 34 (Leban, Kaučič & Rajić, 1993)] – crystal structures have been obtained. Nickel-substituted aluminophosphates have been reported for the first time only very recently (Rajić, Stojaković & Kaučič, 1991). As the aluminophosphate molecular sieves appear to be promising catalytic systems and as nickel complexes (including the Ni-exchanged zeolites) often exhibit high catalytic activity, it seemed likely that Ni-substituted aluminophosphates should also be potentially good catalytic materials.

In this paper we report the crystal structure of $NiAl_3P_4O_{18}C_4H_{21}N_4$, referred to as NiAPO, from single-crystal diffraction data. This is the first crystal structure of an aluminophosphate molecular sieve containing nickel in the framework. Nickel-substituted aluminophosphates can be obtained, but only for structural types where aluminium is coordinated not only in a tetrahedral manner, but also by more than four ligands. $AlPO_4$-21 (Parise & Day, 1985) is known to contain four-, five- and six-coordinate aluminium atoms. Thus, while in CoAPO-21 (Cheetham, Harding, Rizkallah, Kaučič & Rajić, 1991) the Co^{2+} ions replace *tetrahedral* aluminium atoms, Ni^{2+} is expected to replace *octahedral* aluminium atoms in the same type of structure. The principal reason is most likely the much greater tendency of Ni^{II} to form octahedral rather than tetrahedral complexes (West, 1988).

The technical challenge of this crystal sample was twofold. First, the crystals available were small; the one used had dimensions $0.02 \times 0.05 \times 0.25$ mm. To solve this problem a Cu $K\alpha$ rotating-anode diffractometer was used. The use of Cu $K\alpha$ rather than Mo $K\alpha$ radiation increases the scattering efficiency by the ratio of the wavelengths squared [*i.e.* $(1.54178/0.71069)^2 = 4.7$]. As the crystal did not suffer radiation damage, there was no need to extend the sample lifetime by the use of a short wavelength (Helliwell & Fourme, 1983; Helliwell, 1984, p. 1471). The use of a high-power rotating anode also led to a larger fraction of the measured Cu $K\alpha$ data being significant.

The second technical challenge in this study was to pinpoint the site of the Ni-atom incorporation. Between Cu $K\alpha$ and Mo $K\alpha$ wavelengths the dispersive anomalous difference ($\Delta f'$) is 3.32 e for nickel and only 0.15 e for aluminium (Sasaki, 1989). Hence, it was possible to consider the calculation of an f' difference Fourier electron-density map using calculated phases. In our previous study of a chlorine-containing organic molecule ($C_{10}H_{11}NOCl$), the Cl-atom position was deduced from an f' difference Fourier map (Gomez de Anderez *et al.*, 1989). Therefore, in this study, an additional data set was collected using Mo $K\alpha$ radiation and the f' difference Fourier calculation was performed.

2. Experimental

2.1. *Synthesis and chemical analysis of* NiAPO

The reaction gel, prepared by the procedure reported earlier (Rajić, Kaučič & Stojaković, 1990), was of the following composition: $0.4NiO{:}0.8Al_2O_3{:}1.0P_2O_5{:}1.5en{:}50H_2O$ (en = ethylenediamine; the source of nickel was nickel acetate and the source of aluminium was aluminium isopropoxide). Crystallization was carried out in a teflon-lined autoclave under static conditions at 443 K, over 4 days, and yielded blue needle-shaped crystals (Rajić, Stojaković & Kaučič, 1991). Bulk chemical analysis of these crystals gave the approximate composition $(Ni_{0.09}Al_{0.43}P_{0.50})O_2{*}0.25H_2O$, and an IR spectrum of this material exhibited a rather strong band at 1520 cm^{-1}, indicating that some en molecules were present as protonated species.

2.2. Cu $K\alpha$ *data*

A blue needle crystal of $NiAl_3P_4O_{18}C_4H_{21}N_4$, having approximate dimensions $0.02 \times 0.05 \times 0.25$ mm, was mounted on a glass fibre. All measurements were made on a Rigaku AFC-5R diffractometer at 295 K with graphite-monochromated Cu $K\alpha$ radiation and a 12 kW rotating-anode generator. Cell constants and an orientation matrix for data

collection were obtained from least-squares refinement of 25 reflections in the range $75.51 < 2\theta < 79.68°$. ω–2θ scans were performed, the maximum 2θ was 160.1° ($0 \le h \le 11$, $0 \le k \le 18$, $-16 \le l \le 16$), the scan speed was 4.0 or 8.0° min^{-1} (in ω) and weak reflections [$I < 10.0\sigma(I)$] were rescanned (maximum of two rescans). An empirical absorption correction was applied, based on azimuthal scans of three reflections and resulting in transmission factors ranging from 0.78 to 1.00. The data were corrected for Lorentz and polarization effects and a correction for secondary extinction was applied (coefficient = 0.62793×10^{-6}). The intensities of three standard reflections measured after every 150 reflections showed no signs of decay. Further details of the data collection and reduction are contained in Table 1. The structure was solved by direct methods (Sheldrick, 1985). The non-H atoms were refined anisotropically. H atoms bonded to the ethylene diamine ligands were included in idealized positions and those attached to the water molecules were found by difference Fourier synthesis. All were assigned isotropic thermal parameters that were 20% greater than the equivalent B value of the atom to which they were bonded. Full-matrix least-squares refinement of 309 parameters minimized the function $\sum w(|F_o| - |F_c|)^2$, where $w = 4F_o^2/\sigma^2(F_o^2)$ and $\sigma^2(F_o^2) = [S^2(C + R^2B) + (pF_o^2)^2]/\mathrm{Lp}^2$ (S = scan rate, C = total integrated peak count, R = ratio of scan time to background counting time, B = total background count, Lp = Lorentz–polarization factor, and p = 0.03). Neutral-atom scattering factors were used (Cromer & Waber, 1974). Anomalous-dispersion effects were included in F_{calc} (Ibers & Hamilton, 1964). The values for f' and f'' were taken from Cromer (1974). All calculations were performed using the *TEXSAN* crystallographic software package (Molecular Structure Corporation, 1988).*

Table 1. *Experimental details*

(*a*) Crystal data		
Empirical formula	$NiAl_3P_4O_{18}C_4H_{21}N_4$	
Formula weight	676.77	
Crystal colour, habit	Blue, needle	
Crystal dimensions (mm)	0.02 × 0.05 × 0.25	
Crystal system	Monoclinic	
Radiation	Cu $K\alpha$ (λ = 1.54178 Å)	Mo $K\alpha$ (λ = 0.71069 Å)
No. of reflections used for unit-cell determination	25	10
2θ range (°)	75.5–79.7	9.7–14.8
ω-scan peak width at half-height	0.35	0.34
Lattice parameters		
a (Å)	10.0209 (8)	10.03 (2)
b (Å)	15.661 (1)	15.67 (2)
c (Å)	14.0914 (8)	14.14 (2)
β (°)	101.216 (5)	101.3 (1)
V (Å^3)	2169.3 (5)	2180 (5)
Space group	$P2_1/n$ (No. 14)	
Z	4	
D_x (g cm^{-3})	2.062	
F_{000}	1376	
$\mu_{Cu\ K\alpha}$ (cm^{-1})	62.13	13.91
(*b*) Intensity measurements		
Diffractometer	Rigaku AFC-5R	Rigaku AFC-6S
X-ray generator setting	50 kV, 140 mA	50 kV, 30 mA
Temperature (K)	295	296
Scan type	ω–2θ	ω–2θ
Scan rate (in ω) (° min^{-1})	4.0 or 8.0	2.0
No. of rescans	2	3
Scan width (°)	0.94 + 0.30tanθ	0.73 + 0.30tanθ
$2\theta_{max}$ (°)	160.1	50.1
d_{min}	0.78	0.84
No. of reflections measured		
Total	4840	4238
Unique	4601	3997
R_{int}	0.044	0.195
Corrections	Lorentz–polarization Absorption (transmission factors: 0.78–1.00) Secondary extinction (coefficient: 0.62793×10^{-6})	Lorentz–polarization Absorption (transmission factors: 0.93–1.11)
(*c*) Structure solution and refinement		
Structure solution	Direct methods	
H-atom treatment	Included in difference map or calculated positions (d_{C-H} = 0.95 Å)	
Refinement	Full-matrix least squares	
Function minimized	$\sum w(\lvert F_o\rvert - \lvert F_c\rvert)^2$	
Least-squares weights	$4F_o^2/\sigma^2(F_o^2)$	
p factor	0.03	
Anomalous dispersion	All non-H atoms	
No. of observations [with $I > 3.00\sigma(I)$]	3497	1057
No. of parameters	309	177
Reflection/parameter ratio	11.32	5.97
Residuals		
R	0.057	0.050
wR	0.081	0.055
Goodness-of-fit indicator	2.49	1.17
Maximum shift/e.s.d. in final cycle	0.04	< 0.01
Maximum peak in final difference map (e Å^{-3})	0.86	0.51
Minimum peak in final difference map (e Å^{-3})	−0.88	−0.54

2.3. Mo $K\alpha$ *data*

Measurements were made on a Rigaku AFC-6S diffractometer at 296 K, with graphite-monochromated Mo $K\alpha$ radiation, using the same crystal as before; the experimental methods employed in the data collection were essentially the same as those described above and parameters for the data collection and reduction are contained in Table 1. ω–2θ scans were made, with the maximum 2θ being 50.0° ($0 \le h \le 12$, $0 \le k \le 19$, $-17 \le l \le 17$). The intensities of three standard reflections measured after every 150 reflections did not change significantly. An empirical absorption correction was applied using the program *DIFABS* (Walker & Stuart, 1983) and resulted in transmission factors ranging from 0.93 to 1.11. Lorentz and polarization corrections were applied. Refinement was carried out on the solution obtained for the Cu $K\alpha$ data collection. Ni, P and Al atoms were refined anisotropically. All other non-H atoms were refined isotropically. H atoms were treated as described above. Calculations were carried out using the software described above.

* Lists of structure factors, anisotropic thermal parameters and H-atom parameters have been deposited with the British Library Document Supply Centre as Supplementary Publication No. SUP 55806 (79 pp.). Copies may be obtained through The Technical Editor, International Union of Crystallography, 5 Abbey Square, Chester CH1 2HU, England. [CIF reference: LI0137]

2.4. *f′ difference Fourier calculation*

This calculation was performed using the scaled data sets measured at Cu $K\alpha$ and Mo $K\alpha$ wavelengths, to determine at which site incorporation of nickel had taken place. The strategy adopted was to compute a difference Fourier map using the differences between the structure-factor amplitudes determined at both Cu $K\alpha$ and Mo $K\alpha$ wavelengths, along with phases calculated excluding any contribution by the probable Ni atom. Because of the centrosymmetric space group ($P2_1/n$) of the structure, the ($F_{\text{Mo }K\alpha} - F_{\text{Cu }K\alpha}$) difference corresponded only to the real $\Delta f'$ scattering, since the out of phase $\Delta f''$ term is effectively subtracted out. The ratio between the f' differences of the Ni and Al atoms at both wavelengths is nearly 24 [*i.e.* $\Delta f'_{\text{Ni}} = -3.32$ e; $\Delta f'_{\text{Al}} = 0.15$ e (Sasaki, 1989)]. Hence an f' difference Fourier map should give a significant peak at the atom site where Ni has been incorporated. In order to get a suitable phase set to compute f' difference Fourier maps, a refinement of the structure, excluding the Ni atom in the octahedral site, was carried out using *SHELX*76 (Sheldrick, 1976) [2685 independent reflections with $I > 3\sigma(I)$, λ(Cu $K\alpha$), maximum $2\theta = 120°$, all non-H atoms isotropically refined, unit weighting scheme].

The rather large final R factor ($R = 0.36$) is consistent with the fact that some extra scattering contribution, present in the structure, was not taken into account in the refinement. This is clearly reinforced by the occurrence, in the final difference $(F_{\text{calc}} - F_{\text{obs}})_{\text{Cu }K\alpha}$ Fourier synthesis, of a strong peak (located at $x = 0.119$, $y = 0.775$, $z = 0.136$), the magnitude of which (27.4 e) was 8.5 times larger than that of the following strongest peak (3.2 e). At the final stage of the refinement, the average absolute difference $|\Delta\varphi|$ between calculated phases and their exact values obtained when the Ni atom was included in the refinement was found to be 20.9°. A final data set, including 2222 reflections ($0 \le h \le 10$, $0 \le k \le 16$, $-15 \le l \le 15$) for which structure factors at both wavelengths and phases were present, was generated using the *CCP*4 program suite (SERC Daresbury Laboratory, 1986). After scaling on F^2, the scale factor between the Cu $K\alpha$ and Mo $K\alpha$ structure factors, expressed *versus* resolution, was found to be $0.994\,(\pm 0.0159) + 0.00187\,(\pm 0.0346)\sin^2\theta/\lambda^2$. The corresponding mean fractional isomorphous difference $\langle \Delta F/F \rangle$ was 0.137.

The subsequent f' difference Fourier map, computed taking into account 2178 reflections for which $|F_{\text{Mo }K\alpha} - F_{\text{Cu }K\alpha}|$ was less than 3.5 times the mean difference, is shown in Fig. 1. The highest peak (the height of which was six times the r.m.s. value), was located at $x = 0.140$, $y = 0.762$, $z = 0.082$, a position that, according to the symmetry-related Ni-atom position deduced from the final structure refinement, was in fact displaced by 0.82 Å. This result corroborates the previous analysis of the $(F_{\text{calc}} - F_{\text{obs}})_{\text{Cu }K\alpha}$ Fourier map obtained after a crude refinement, omitting the inclusion of any atom at the six-coordinate site. Even if it does not uniquely establish the nature of the atom present at this site, it reinforces the fact that it has to be a heavier atom than an Al-atom, as the small $\Delta f'_{\text{Al}}$ value could not induce such a well defined peak.

In order to check this latter assumption, two other phase sets and their resulting difference maps were calculated. In the first, not only the Ni atom, but also an Al atom [Al(1)] were omitted in a new refinement of the structure. The R value was 0.41; two peaks, the heights of which were 29.2 e and 16.2 e (the intensity of the next highest peak was less than 1 e), were observed at $x = 0.119$, $y = 0.773$, $z = 0.136$ and $x = 0.274$, $y = 0.121$, $z = 0.774$, respectively, in the final $(F_{\text{calc}} - F_{\text{obs}})$ map. The $|\Delta\varphi|$ value, between this new phase set and the one including all the atoms, was 24°. An analysis of the corresponding f' difference map clearly indicated only one main peak (the height of which was five times the r.m.s. value), located at $x = 0.109$, $y = 0.760$, $z = 0.136$, a position distant from the refined Ni-atom site by only 0.21 Å. The next highest peak (half the height of the previous one) could not be related to either Al(1) or to any other atomic position in the structure.

When the three Al atoms and the Ni atom were excluded from the phase calculation (R factor 0.48, $|\Delta\varphi| = 31.9°$), the highest peak was still found at the Ni-atom site, but the peak height was slightly lowered (4.25 times the r.m.s. value). The next highest peak (3.25 the r.m.s. value), located at $x = 0.714$, $y = 0.386$, $z = 0.285$, was found at 0.61 Å from the Al(1) position. No residual density was found at the Al(2) or Al(3) sites. So, in all the f' difference Fourier maps the highest peak always occurred at the putative Ni-atom site.

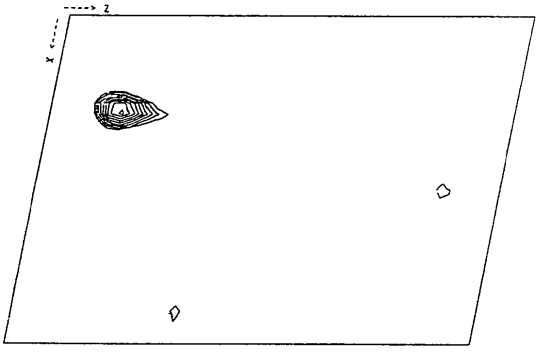

Fig. 1. Difference Fourier map ($y = 0.76$) containing the expected Ni-atom peak. The contour interval is 0.5 r.m.s., starting at 2.25 r.m.s.

3. Results and discussion

3.1. *Description of the structure*

The asymmetric unit of the structure includes one Ni, three Al, four P and 16 framework O atoms (Fig. 2). In addition there are two ethylenediamine fragments and two water molecules. Atom coordinates are shown in Table 2 and bond distances and angles in Table 3. The structure consists of aluminophosphate layers bridged by Ni atoms (Fig. 3). In the aluminophosphate layers, the Al and P atoms occupy tetrahedral positions. There are two classes of phosphorus–oxygen bond in the structure. In the first are P—(O—Al) bonds with a mean distance of 1.485 (4) Å. In the second are P—(O—Ni) and terminal P—O bonds with a mean distance of 1.542 (4) Å.

The Ni atoms reside in slightly distorted octahedral sites. Each atom is linked to the aluminophosphate layer on either side by an O atom (Fig. 4). The octahedron is completed by one water molecule [O(3)] and two ethylenediamine templates, one of which is monodentate and the other bidentate. The bond distances to Ni are within the expected limits for an Ni-atom bonded to framework O atoms, OH_2 and the N atoms of a primary amine. The uncoordinated N atom of the monodentate ethylenediamine is protonated. It forms hydrogen bonds to the aluminophosphate layers and the free water molecule between them (Table 4). The torsion angle about the C(3)—C(4) bond is 65.2 (8)°. The bidentate template molecule and the Ni atom are arranged in a distorted envelope shape. C(2) is −0.6 Å out of the plane formed by N(2), Ni(1), N(1) and C(1); the mean deviation from the plane by these atoms is 0.06 Å. The free water molecule [O(18)] has higher thermal parameters than the other non-H atoms as it is only held to the rest of the structure by hydrogen bonding.

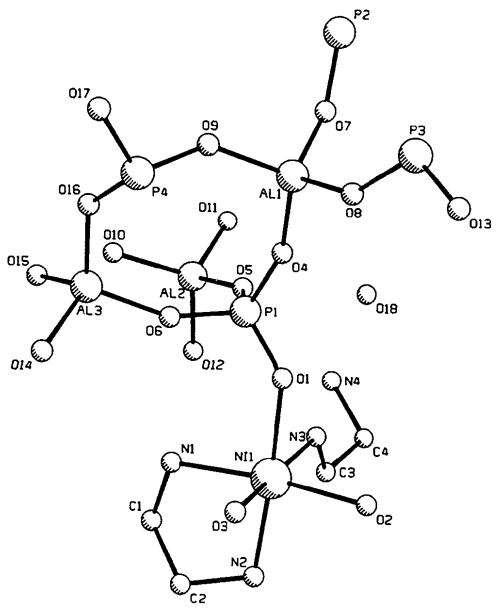

Fig. 2. The asymmetric unit, with H atoms omitted, viewed down the *b* axis and showing the atom-numbering scheme.

Table 2. *Positional parameters and* B_{eq} *values for* NiAPO

The first line gives the values derived from the AFC-5R data, the second line gives those derived from the AFC-6S data.

$B_{eq} = (8\pi^2/3)\sum_i\sum_j U_{ij} a_i^* a_j^* \mathbf{a}_i.\mathbf{a}_j.$

	x	*y*	*z*	B_{eq} (Å^2)
Ni(1)	−0.8828 (1)	0.77237 (7)	0.13402 (7)	1.33 (4)
	−0.8826 (2)	0.7721 (1)	0.1344 (2)	1.1 (1)
P(1)	−0.5492 (1)	0.7934 (1)	0.1421 (1)	0.98 (5)
	−0.5501 (4)	0.7931 (3)	0.1420 (3)	0.7 (2)
P(2)	−0.0018 (1)	0.7851 (1)	0.3401 (1)	0.97 (5)
	−0.0019 (4)	0.7858 (3)	0.3396 (3)	1.0 (2)
P(3)	−0.2295 (1)	0.9938 (1)	0.4387 (1)	1.15 (5)
	−0.2296 (5)	0.9939 (3)	0.4386 (4)	1.0 (2)
P(4)	−0.2729 (1)	0.9840 (1)	0.0741 (1)	1.14 (5)
	−0.2738 (5)	0.9840 (3)	0.0736 (4)	1.0 (2)
Al(1)	−0.2759 (2)	0.8785 (1)	0.2572 (1)	1.05 (6)
	−0.2755 (5)	0.8783 (3)	0.2576 (4)	0.7 (2)
Al(2)	−0.5031 (2)	0.6232 (1)	0.0365 (1)	1.07 (6)
	−0.5036 (5)	0.6239 (3)	0.0367 (4)	0.8 (2)
Al(3)	−0.4985 (2)	0.8851 (1)	−0.0500 (1)	1.09 (6)
	−0.4984 (6)	0.8850 (3)	−0.0509 (4)	1.1 (2)
O(1)	−0.6763 (4)	0.8014 (3)	0.1806 (3)	1.6 (2)
	−0.678 (1)	0.8023 (7)	0.1811 (7)	1.2 (2)
O(2)	−0.9175 (4)	0.8098 (3)	0.2690 (3)	1.7 (2)
	−0.914 (1)	0.8088 (7)	0.2690 (8)	1.5 (2)
O(3)	−0.9164 (5)	0.9037 (3)	0.1044 (3)	2.1 (2)
	−0.914 (1)	0.9040 (7)	0.1047 (9)	1.8 (2)
O(4)	−0.4284 (4)	0.8280 (3)	0.2150 (3)	1.7 (2)
	−0.430 (1)	0.8291 (8)	0.2150 (8)	1.6 (2)
O(5)	−0.5145 (5)	0.6988 (3)	0.1245 (3)	1.8 (2)
	−0.516 (1)	0.7009 (7)	0.1235 (8)	1.4 (2)
O(6)	−0.5582 (5)	0.8395 (3)	0.0451 (3)	2.0 (2)
	−0.559 (1)	0.8409 (8)	0.0465 (8)	1.3 (2)
O(7)	−0.1539 (4)	0.8028 (3)	0.3049 (3)	1.7 (2)
	−0.154 (1)	0.8031 (7)	0.3058 (7)	1.2 (2)
O(8)	−0.3035 (4)	0.9521 (3)	0.3438 (3)	1.6 (2)
	−0.305 (1)	0.9526 (8)	0.3437 (8)	1.2 (2)
O(9)	−0.2193 (4)	0.9236 (3)	0.1600 (3)	1.9 (2)
	−0.219 (1)	0.9240 (8)	0.159 (1)	2.1 (3)
O(10)	−0.4537 (4)	0.6668 (3)	−0.0642 (3)	1.6 (2)
	−0.451 (1)	0.6666 (8)	−0.0649 (8)	1.6 (2)
O(11)	−0.3900 (4)	0.5454 (3)	0.0874 (3)	1.6 (2)
	−0.387 (1)	0.5454 (8)	0.0877 (8)	1.6 (2)
O(12)	−0.6663 (4)	0.5800 (3)	0.0071 (3)	1.8 (2)
	−0.665 (1)	0.5804 (7)	0.0073 (8)	1.3 (2)
O(13)	−0.3197 (4)	1.0468 (3)	0.4863 (3)	2.0 (2)
	−0.320 (1)	1.0462 (8)	0.4846 (8)	1.5 (2)
O(14)	−0.6121 (5)	0.9628 (3)	−0.1031 (3)	1.9 (2)
	−0.610 (1)	0.9632 (8)	−0.101 (1)	2.0 (3)
O(15)	−0.4886 (4)	0.8108 (3)	−0.1387 (3)	1.6 (2)
	−0.488 (1)	0.8106 (7)	−0.1383 (8)	0.9 (2)
O(16)	−0.3367 (4)	0.9282 (3)	−0.0138 (3)	2.1 (2)
	−0.336 (1)	0.9279 (8)	−0.0138 (9)	1.6 (2)
O(17)	−0.1579 (5)	1.0368 (3)	0.0532 (3)	2.3 (2)
	−0.156 (1)	1.0349 (8)	0.052 (1)	2.4 (3)
O(18)	−0.5344 (6)	0.5826 (4)	0.2850 (4)	4.0 (3)
	−0.536 (2)	0.5826 (9)	0.284 (1)	3.5 (3)
N(1)	−0.8647 (6)	0.7506 (4)	−0.0108 (4)	2.1 (2)
	−0.866 (2)	0.749 (1)	−0.009 (1)	2.4 (3)
N(2)	−1.0907 (5)	0.7464 (4)	0.0777 (4)	2.0 (2)
	−1.089 (1)	0.746 (1)	0.077 (1)	2.3 (3)
N(3)	−0.8229 (6)	0.6497 (4)	0.1861 (4)	2.1 (2)
	−0.824 (1)	0.650 (1)	0.185 (1)	2.0 (3)
N(4)	−0.7410 (6)	0.4607 (4)	0.1906 (4)	2.2 (2)
	−0.746 (1)	0.460 (1)	0.192 (1)	1.3 (3)
C(1)	−0.9954 (7)	0.7163 (5)	−0.0644 (5)	2.8 (3)
	−0.994 (2)	0.713 (1)	−0.066 (1)	2.2 (4)
C(2)	−1.1107 (7)	0.7575 (5)	−0.0283 (5)	2.5 (3)
	−1.110 (2)	0.757 (1)	−0.026 (1)	2.1 (4)
C(3)	−0.9149 (7)	0.5765 (4)	0.1774 (5)	2.0 (2)
	−0.912 (2)	0.576 (1)	0.178 (1)	2.1 (4)
C(4)	−0.8563 (7)	0.4962 (5)	0.2315 (5)	2.2 (3)
	−0.855 (2)	0.494 (1)	0.231 (1)	1.7 (4)

Table 3. *Intramolecular distances* (Å) *and angles* (°) *for* NiAPO

(*a*) Intramolecular distances from AFC-5R data

Ni(1)—O(1)	2.096 (4)	P(4)—O(16)	1.549 (4)
Ni(1)—O(2)	2.083 (4)	P(4)—O(17)	1.493 (4)
Ni(1)—O(3)	2.112 (5)	Al(1)—O(4)	1.721 (4)
Ni(1)—N(1)	2.111 (5)	Al(1)—O(7)	1.741 (5)
Ni(1)—N(2)	2.120 (5)	Al(1)—O(8)	1.741 (4)
Ni(1)—N(3)	2.102 (6)	Al(1)—O(9)	1.731 (4)
P(1)—O(1)	1.483 (4)	Al(2)—O(5)	1.733 (4)
P(1)—O(4)	1.527 (4)	Al(2)—O(10)	1.732 (4)
P(1)—O(5)	1.552 (4)	Al(2)—O(11)	1.723 (4)
P(1)—O(6)	1.533 (4)	Al(2)—O(12)	1.744 (4)
P(2)—O(2')	1.482 (4)	Al(3)—O(6)	1.726 (5)
P(2)—O(7)	1.533 (4)	Al(3)—O(14)	1.734 (4)
P(2)—O(10")	1.538 (4)	Al(3)—O(15)	1.725 (4)
P(2)—O(15")	1.533 (4)	Al(3)—O(16)	1.738 (5)
P(3)—O(8)	1.543 (4)	N(1)—C(1)	1.480 (9)
P(3)—O(11"')	1.547 (4)	N(2)—C(2)	1.479 (8)
P(3)—O(12")	1.559 (5)	N(3)—C(3)	1.461 (8)
P(3)—O(13)	1.480 (4)	N(4)—C(4)	1.494 (8)
P(4)—O(9)	1.548 (4)	C(1)—C(2)	1.50 (1)
P(4)—O(14")	1.540 (4)	C(3)—C(4)	1.53 (1)

(*b*) Range of bond angles at tetrahedral atoms

P(1)	105.9 (3)–112.3 (2)	Al(1)	105.6 (2)–113.9 (2)
P(2)	106.4 (3)–113.3 (2)	Al(2)	104.2 (2)–112.7 (2)
P(3)	106.2 (2)–113.4 (2)	Al(3)	106.6 (2)–112.2 (2)
P(4)	106.7 (2)–113.5 (3)		

(*c*) Selected intramolecular bond angles

O(1)—Ni(1)—O(2)	89.0 (2)	P(1)—O(5)—Al(2)	144.5 (3)
O(1)—Ni(1)—O(3)	87.7 (2)	P(1)—O(6)—Al(3)	156.7 (3)
O(1)—Ni(1)—N(1)	94.2 (2)	P(2)—O(7)—Al(1)	145.8 (3)
O(1)—Ni(1)—N(2)	176.2 (2)	P(3)—O(8)—Al(1)	140.7 (3)
O(1)—Ni(1)—N(3)	83.8 (2)	P(4)—O(9)—Al(1)	138.6 (3)
O(2)—Ni(1)—O(3)	81.8 (2)	P(2") —O(10)—Al(2)	145.2 (3)
O(2)—Ni(1)—N(1)	171.4 (2)	P(3"') —O(11)—Al(2)	138.4 (3)
O(2)—Ni(1)—N(2)	94.0 (2)	P(3") —O(12)—Al(2)	133.2 (3)
O(2)—Ni(1)—N(3)	91.5 (2)	P(4") —O(14)—Al(3)	136.7 (3)
O(3)—Ni(1)—N(1)	90.3 (2)	P(2") —O(15)—Al(3)	142.0 (3)
O(3)—Ni(1)—N(2)	90.3 (2)	P(4)—O(16)—Al(3)	132.1 (3)
O(3)—Ni(1)—N(3)	169.3 (2)	Ni(1)—N(1)—C(1)	108.5 (4)
N(1)—Ni(1)—N(2)	82.5 (2)	Ni(1)—N(2)—C(2)	106.6 (4)
N(1)—Ni(1)—N(3)	96.8 (2)	Ni(1)—N(3)—C(3)	123.7 (4)
N(2)—Ni(1)—N(3)	98.5 (2)	N(1)—C(1)—C(2)	109.6 (6)
Ni(1)—O(1)—P(1)	137.1 (3)	N(2)—C(2)—C(1)	109.3 (6)
Ni(1)—O(2)—P(2')	139.7 (3)	N(3)—C(3)—C(4)	115.4 (5)
P(1)—O(4)—Al(1)	158.5 (3)	N(4)—C(4)—C(3)	111.4 (5)

Symmetry codes: (i) $-1+x, y, z$; (ii) $-\frac{1}{2}+x, \frac{3}{2}-y, -\frac{1}{2}+z$; (iii) $-\frac{1}{2}-x, -\frac{1}{2}+y, \frac{1}{2}-z$; (iv) $-1-x, 2-y, -z$.

3.2. *Comparison of* NiAPO *with other aluminophosphates*

The preparation of NiAPO was analogous to that of CoAPO-21 (Cheetham, Harding, Rizkallah, Kaučič & Rajić, 1991) except that the reaction mixture contained nickel acetate instead of cobalt acetate. Initial expectations were that the framework structure would be of the $AlPO_4$-21 type, since in the case of doping with Co, 6% Co was incorporated into a tetrahedral aluminium site leaving the $AlPO_4$-21 structure basically unchanged. However, the cell dimensions were quite different to those of CoAPO-21 (Cheetham, Harding, Rizkallah, Kaučič & Rajić, 1991), and determination of the NiAPO structure has shown that a totally novel structure has been formed, in which nickel appears to occupy the octahedral site almost exclusively.

The bond lengths to the Ni atom are all within acceptable limits, and in particular are longer than would be expected for six-coordinate aluminium (Parise & Day, 1985; Cheetham, Harding, Rizkallah, Kaučič & Rajić, 1991; Helliwell *et al.*, 1993). Moreover, spectroscopic studies on NiAPO suggest that octahedral nickel is present, coordinated to water and nitrogen donors, clearly in agreement with the crystallographic evidence (Rajić, Stojaković & Kaučič, 1991).

The temperature factor for Ni(1) [B_{eq} = 1.33 (4) Å^2, for the Cu $K\alpha$ determination] is a little higher than those of the three Al atoms, whose temperature factors are all very similar, with B_{eq} ranging from 1.05 (6) to 1.09 (6) Å^2 for the Cu $K\alpha$ data. This could be explained by the fact that only two of the atoms within the coordination sphere of Ni(1) are framework atoms, the remaining four being from the en and water ligands, whereas all the Al atoms are tetrahedrally bound to framework O atoms. Another explanation could be that there is some aluminium at this site. In order to determine

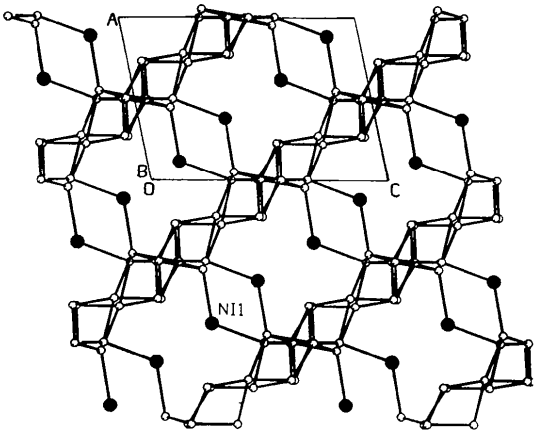

Fig. 3. The crystal structure viewed down the *b* axis. H, O, N and C atoms have been omitted for clarity. The filled circles are Ni atoms.

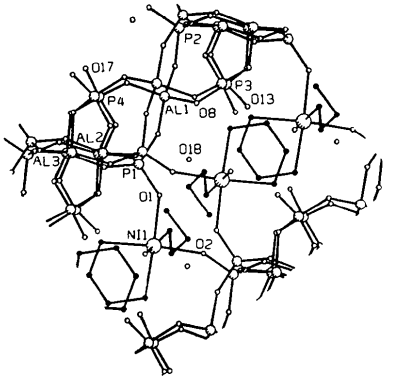

Fig. 4. The section of the crystal structure viewed down the *b* axis. The filled circles represent template N and C atoms. H atoms have been omitted.

Table 4. *Intermolecular distances below* 3.2 Å, *assumed to be hydrogen bonds*

O(2)—N(4^{i})	2.843 (7)	O(17)—O(18^{ii})	2.777 (7)
O(3)—O(17^{iii})	3.170 (7)	O(18)—N(4)	2.937 (8)
O(5)—O(18)	2.941 (7)		

Symmetry codes: (i) $-\frac{1}{2}-x, \frac{1}{2}+y, \frac{1}{2}-z$; (ii) $-\frac{1}{2}-x, \frac{1}{2}+y, \frac{1}{2}-z$; (iii) $-1+x, y, z$.

the possible aluminium content, the Ni(1) site was treated as $[x\text{Al} + (1-x)\text{Ni}]$, with its B_{eq} fixed at the average of that of the three Al atoms. Refinement of x converged to $x = 0.087\,(6)$ for the Cu $K\alpha$ data. From the Mo $K\alpha$ data, a value of 0.040 (9) was obtained. Bulk analyses of this sample were performed several times, and certainly showed that nickel was present in approximately the expected proportion. However, the results varied too much to ascertain whether there was any aluminium at the Ni-atom site. Hence, we conclude that nickel has been incorporated at this site almost exclusively but that there might also be up to 10% aluminium present.

The binding of the ethylenediamine ligand to the Ni atom through an N atom is unusual, since the template molecules for aluminophosphate lattices normally reside within the pores and are hydrogen bonded to the framework. When NiAPO is heated to temperatures above 493 K, oxidation of the organic component takes place and leads to the collapse of the crystal structure to an amorphous material, presumably due to the removal of en and water ligands from nickel. For CoAPO-21, en is disordered over two sites within the pores. Therefore, removal of en with heat takes place without collapse of the crystal structure. However, calcination of CoAPO-21 above 673 K leads to a change of the structural type and CoAPO-25 is obtained. This is in agreement with the observed transformation of the $AlPO_4$-21 structural type to $AlPO_4$-25 with calcination in air (Wilson, Lok & Flaningen, 1982).

The positional parameters obtained as a result of the AFC-5R and AFC-6S data collections are the same, within experimental error, although due to the weakness of the Mo $K\alpha$ data set the e.s.d.'s of the parameters are higher (see Table 5). The temperature factors resulting from the Mo $K\alpha$ data set are generally lower than those derived from the Cu $K\alpha$ data set. For non-H atoms, $B_{Mo}/B_{Cu} = 0.86$. This also is probably because of the weakness of the Mo $K\alpha$ data set, which results in an over-estimation of the reflection intensities at high angles because of noise contributions.

The weakness of the Mo $K\alpha$ data set *versus* the Cu $K\alpha$ data set is exemplified by comparing the number of data with $I > 3\sigma(I)$ in each case. For Mo $K\alpha$, 1057 reflections were considered observed, out of 3997 unique reflections measured. For Cu $K\alpha$, 3497 reflections were observed (using the same criterion) out of 4601 unique reflections measured. The high proportion of observed data obtained with the AFC-5R at Cu $K\alpha$ is much in line with results obtained for CrAPO-14 and SAPO-43 (Helliwell *et al.*, 1993). In order to compare samples, it is useful to calculate their scattering efficiencies. We can obtain a measure of the scattering efficiency of a particular sample by use of the formula (Andrews *et al.*, 1988):

$$\text{Scattering efficiency} = \left(\sum_{i=1}^{N} n_i f_i^2\right)\frac{V_x}{V_o^2}\ (\text{e}^2\ \text{Å}^{-3}),$$

where f_i is the atomic number of the ith atom type; n_i is the number of atoms of that type in a cell; N is the number of atom types in a cell; V_x is the sample volume; V_o is the cell volume. Table 6 shows scattering efficiencies of the crystal samples used in the NiAPO, CrAPO-14 and SAPO-43 studies.

The scattering efficiency of NiAPO is about the same as that of CrAPO-14 and four times that of SAPO-43. In all cases, acceptable numbers (50–100) of reflections per atom were obtained with data collections using the AFC-5R (103, 121 and 91, respectively). In fact, we have successfully collected data on the AFC-5R from samples whose scattering efficiencies are down to about 1/8 that of NiAPO, provided the crystal quality is otherwise good, as it is for these samples (see Table 1 for ω-scan peak width at half-height). By contrast, our experience has shown that reasonable reflection/atom ratios are usually obtained on the AFC-6S with an Mo $K\alpha$ sealed tube on crystals of about ten times or more the scattering efficiency of NiAPO. Clearly, data collection on NiAPO using the AFC-6S is at the

Table 5. *Differences between the coordinates obtained from the* Cu $K\alpha$ *and* Mo $K\alpha$ *data and a comparison of their e.s.d.'s*

		x	y	z
Ni atom	Difference × 10^4	2	4	4
	E.s.d. × 10^4 (Cu $K\alpha$)	1	1	1
	E.s.d. × 10^4 (Mo $K\alpha$)	2	1	2
Al and P atoms	Mean difference × 10^4	4	3	4
	Maximum difference × 10^4	9	7	9
	E.s.d. × 10^4 (Cu $K\alpha$)	1	1	1
	E.s.d. × 10^4 (Mo $K\alpha$)	5	3	4
C, N and O atoms	Mean difference × 10^4	17	8	9
	Maximum difference × 10^4	50	33	23
	E.s.d. × 10^4 (Cu $K\alpha$)	5	3	4
	E.s.d. × 10^4 (Mo $K\alpha$)	12	8	9

Table 6. *Comparison of scattering efficiencies of aluminophosphate samples mentioned in the text*

Sample	Sample volume, V, (μm^3)	Sample scattering efficiency (e^2 Å^{-3})
NiAPO	25 × 10^4	787 × 10^{12}
CrAPO-14*	12 × 10^4	829 × 10^{12}
SAPO-43*	75 × 10^3	208 × 10^{12}

* See Helliwell *et al.* (1993).

limits of experimental feasibility, yielding a data/atom ratio of 31, and therefore errors on the parameters are necessarily larger.

However, NiAPO data collection on the AFC-6S was carried out in order to compute f'' difference maps. Despite the weakness of the data, we obtained useful results. These show that even if one or all of the Al atoms, together with the Ni atom, are excluded from the phase calculations, the highest peak is unambiguously found at (or very close to) the six-coordinate site, confirming the presence of a metal atom of significant $\Delta f''$ value, such as an Ni atom.

The Ni-atom positions deduced from the $\Delta f''$ analyses were slightly displaced from the refined positions. This is probably due to uncertainties in the phases, because some scattering information was excluded from their calculations, and/or inaccuracies in the Mo $K\alpha$ data set arising from its low intensity. When the Ni atom and all the Al atoms were removed from the calculation of the phases, the highest peak was observed close to the Ni(1) site but an unexpected weaker peak was also seen near the Al(1) site. The probable explanation for this unexpected peak is that because a larger amount of scattering information was excluded from the calculation of the phases, the resulting errors were higher. Evidence for this is given by the value of $|\Delta\varphi|$ (the average absolute difference between the calculated phases and the values obtained from the refinement including all the atoms), which is considerably higher, at 31.9°, than when only Ni(1), or Ni(1) and Al(1) are excluded from the phase calculation ($|\Delta\varphi|$ is 20.9 or 24°).

To elucidate the nickel substitution further, a synchrotron experiment is needed. New sets of data are to be collected at the Ni K edge ($\sim$1.488 Å) to optimize the $\Delta f''_{Ni}$ signals ($\Delta f''_{Ni} = -5.04$ e between $\sim$1.488 Å and Cu $K\alpha$).

4. Concluding remarks

The structure presented is the first of a nickel aluminophosphate. It is of a new type, different from CoAPO-21, which it might have been expected to resemble. Incorporation of the Ni atom in the aluminophosphate structure took place only at the site which had an octahedral environment. The aluminium sites had a tetrahedral environment and so nickel substitution was unlikely (West, 1988).

Technically, the advent of the high-power rotating-anode diffractometer is an important development. When this high-intensity advantage is combined with the use of longer wavelengths (Cu $K\alpha$), the strength of X-ray reflections can be greatly enhanced. Hence, crystals can be studied that are of smaller volume and lower scattering efficiency than those that can normally be studied with an Mo $K\alpha$ sealed-tube diffractometer.

These developments in the home laboratory will certainly push synchrotron efforts in the direction of even weaker scattering cases, especially much smaller crystal volumes. However, zeolites and the aluminophosphates are an important class of sample within chemical crystallography. Clearly, many of these crystals have now come in range of the home machine, which, of course, is very convenient. The use of two wavelengths (Cu $K\alpha$ and Mo $K\alpha$) allowed a sufficient change to the nickel scattering to offer an alternative method of pinpointing its position. It is also true, however, that synchrotron radiation studies exploiting the tunability of the beam to probe more precisely the anomalous-dispersion effects of *specific elements* offer a new and exciting method of structure analysis whether or not the sample volume is expecially small.

The Science and Engineering Research Council (SERC) is thanked for funding the purchase of the Rigaku AFC-5R rotating-anode diffractometer, housed in the Department of Chemistry of the University of Manchester, *via* a research grant to JRH. The Rigaku AFC-6S was funded jointly by UMIST and the University of Manchester and is housed in the UMIST Chemistry Department. The Royal Society is thanked for salary support of BG and for funding the Agreement on Research between Manchester and Ljubljana. Dr M. M. Harding is thanked for discussions. The University of Manchester is thanked for general support.

References

ANDREWS, S. J., PAPIZ, M. Z., MCMEEKING, R., BLAKE, A. J., LOWE, B. M., FRANKLIN, K. R., HELLIWELL, J. R., HARDING, M. M. (1988). *Acta Cryst.* B**44**, 73–77.

BENNETT, J. M., DYTRYCH, W. J., PLUTH, J. J., RICHARDSON, J. W. & SMITH, J. W. (1986). *Zeolites*, **6**, 349–360.

BENNETT, J. M. & MARCUS, B. K. (1988). *Stud. Surf. Sci. Catal.* **37**, 269–279.

CHEETHAM, G. M. T., HARDING, M. M., RIZKALLAH, P. J., KAUČIČ, V. & RAJIĆ, N. (1991). *Acta Cryst.* C**47**, 1361–1364.

CROMER, D. T. (1974). *International Tables for X-ray Crystallography*, Vol. IV, Table 2.3.1. Birmingham: Kynoch Press. (Present distributor Kluwer Academic Publishers, Dordrecht.)

CROMER, D. T. & WABER, J. T. (1974). *International Tables for X-ray Crystallography*, Vol. IV, Table 2.2*A*. Birmingham: Kynoch Press. (Present distributor Kluwer Academic Publishers, Dordrecht.)

GOMEZ DE ANDEREZ, D., HELLIWELL, M., HABASH, J., DODSON, E. J., HELLIWELL, J. R., BAILEY, P. D. & GAMMON, R. E. (1989). *Acta Cryst.* B**45**, 482–488.

HELLIWELL, J. R. (1984). *Rep. Prog. Phys.* **47**, 1403–1497.

HELLIWELL, J. R. & FOURME, R. (1983). *Design Study for the Proposed European Synchrotron Radiation Facility*. Report presented to the Instrumentation Sub Group of the ESRF Ad-hoc Committee on Synchrotron Radiation.

HELLIWELL, M., KAUČIČ, V., CHEETHAM, G. M. T., HARDING, M. M., KARIUKI, B. M. & RIZKALLAH, P. J. (1993). *Acta Cryst.* B49, 413–420.
IBERS, J. A. & HAMILTON, W. C. (1964). *Acta Cryst.* **17**, 781–782.
LEBAN, V., KAUČIČ, V. & RAJIĆ, N. (1993). In preparation.
Molecular Structure Corporation (1988). *TEXSAN. TEXRAY Structure Analysis Package*. Version 2.1. MSC, 3200A Research Forest Drive, The Woodlands, TX 77381, USA.
PARISE, J. B. & DAY, C. S. (1985). *Acta Cryst.* C41, 515–520.
PLUTH, J. J., SMITH, J. V. & RICHARDSON, J. W. (1988). *J. Phys. Chem.* **92**, 2734–2738.
RAJIĆ, N., KAUČIČ, V. & STOJAKOVIĆ, D. (1990). *Zeolites*, **10**, 169–173.
RAJIĆ, N., STOJAKOVIĆ, D. & KAUČIČ, V. (1991). *Zeolites*, **11**, 612–616.
SASAKI, S. (1989). KEK Report 88-14. National Laboratory for High Energy Physics, Tsukuba, Japan.
SERC Daresbury Laboratory (1986). *CCP4. A Suite of Programs for Protein Crystallography*. SERC Daresbury Laboratory, Warrington, England.
SHELDRICK, G. M. (1976). *SHELX*. Program for crystal structure determination. Univ. of Cambridge, England.
SHELDRICK, G. M. (1985). *SHELXS*. In *Crystallographic Computing* 3, edited by G. M. SHELDRICK, C. KRÜGER & R. GODDARD, pp. 175–189. Oxford Univ. Press.
WALKER, N. & STUART, D. (1983). *Acta Cryst.* A39, 158–166.
WEST, A. R. (1988). *Basic Solid State Chemistry*, p. 105. Chichester: John Wiley.
WILSON, S. T., LOK, B. M. & FLANINGEN, E. M. (1982). US Patent No. 4 310 440.

Acta Cryst. (1993). B49, 428–435

Structure of Anhydrous Titanyl Sulfate, Titanyl Sulfate Monohydrate and Prediction of a New Structure

BY B. M. GATEHOUSE* AND S. N. PLATTS

Chemistry Department, Monash University, Clayton, Victoria 3168, *Australia*

AND T. B. WILLIAMS

CSIRO Division of Materials Science and Technology, Normanby Road, Clayton, Victoria 3168, *Australia*

(*Received* 31 *July* 1992; *accepted* 16 *December* 1992)

Abstract

(1) Titanyl sulfate, $TiOSO_4$, $M_r = 159.96$, orthorhombic, $P2_1ma$, $a = 10.942$ (1), $b = 5.158$ (1), $c = 25.726$ (2) Å, $U = 1452.0$ (3) Å^3, D_m (flotation) = 2.96 (2), $D_x = 2.93$ (1) g cm^{-3}, $Z = 16$, λ(Mo $K\alpha$) = 0.7107 Å, $\mu = 23.46$ cm^{-1}, $F(000) = 1248$, $T = 293$ K, final $R = 0.168$ for 2333 counter reflections. A combined X-ray and transmission electron microscopy study allowed the determination and refinement of this structure on a supercell of WPO_5 (a and b equal those above but c is $4 \times c$). The structure consists of an infinite array of corner-shared octahedra and tetrahedra and Ti—O distances range from 1.70 (2) to 2.05 (1) Å. (2) Titanyl sulfate monohydrate, $TiOSO_4.H_2O$, $M_r = 177.97$, orthorhombic, $P2_12_12_1$, $a = 9.818$ (1), $b = 5.133$ (1), $c = 8.614$ (2) Å, $U = 434.1$ (2) Å^3, $Z = 4$, D_m (flotation) = 2.71 (1), $D_x = 2.72$ (1) g cm^{-3}, λ(Mo $K\alpha$) = 0.7107 Å, $\mu = 23.46$ cm^{-1}, $F(000) = 352$, $T = 293$ K, final $R = 0.0190$ for 1985 counter reflections. The structure consists of $[TiO]_n^{2n+}$ chains parallel to the crystallographic b axis linked by sulfate tetrahedra to form the three-dimensional structure. The titanyl bridge is asymmetric [1.6870 (9) and 1.9641 (8) Å] and Ti—O distances range from 1.687 to 2.136 Å. A new structure derived from that of titanyl sulfate hydrate is predicted.

Introduction

As part of a general study of transition-element sulfate complexes (Gatehouse & Platts, 1993) interest focussed on titanyl sulfate ($TiOSO_4$) and its hydrates. These materials have been the subject of several studies as outlined in an earlier report (Naka, Tanaka, Suwa & Takeda, 1977) in which the unit-cell dimensions of $TiOSO_4$, from Weissenberg photographs, and a refinement of its powder diffraction pattern were given.

A structure determination of the monohydrate, $TiOSO_4.H_2O$, was reported some years ago (Lundgren, 1956), with the comments that the 'experimental intensity material was too poor to allow a complete structure determination' and that an 'idealised structure which should be slightly distorted according to $P2_12_12_1$' was being reported. This structure was, nevertheless, essentially the correct one. It has been claimed that a low-temperature or α-$TiOSO_4.H_2O$ can be prepared that is converted into the above form at about 403 K (Pervushin, Tolchev, Denisova, German & Kleshchev, 1989).

Observations on the structure of the dihydrate, $TiOSO_4.2H_2O$, have been reported (Reynolds &

* Author to whom correspondence should be addressed.

0108-7681/93/030428-08$06.00